Increased P-glycoprotein expression in mitochondria is related to acquired multidrug resistance in human hepatoma cells depleted of mitochondrial DNA

XIANLONG LING*, YUQI HE*, GUOQIAO ZHANG, YUAN ZHOU and BIN YAN

Department of Gastroenterology, Xinqiao Hospital, Third Military Medical University, Chongqing 400037, P.R. China

Received June 30, 2011; Accepted August 4, 2011

DOI: 10.3892/ijo.2011.1181

Abstract. Mitochondrial DNA-depleted ϱ^0 cells are resistant to apoptosis, but the mechanism remains unclear. A human hepatoma cell line (SK-Hep1) depleted of mtDNA (ϱ^0SK-Hep1) was induced by ethidium bromide treatment. The ϱ^0SK-Hep1 cells were resistant to both doxorubicin- and cisplatin-induced apoptosis, while cybrids (SK-Hep1Cyb) prepared by fusing ϱ^0SK-Hep1 cells with platelets showed restored susceptibility to both drugs. We observed P-glycoprotein and MRP1 were both overexpressed in ϱ^0 cells, and more P-glycoproteins were localized in the mitochondria and were functionally active. ϱ^0 cells showed resistance to chemotherapeutic drug-induced apoptosis. The increased expression and localization of P-glycoproteins in the mitochondria of ϱ^0 cells may facilitate the exclusion of chemotherapeutic drugs from the mitochondria to the cytosol.

Introduction

Mitochondria are dynamic organelles that play a key role in cellular metabolism. They are sites where key cellular processes occur, such as oxidative decarboxylation of pyruvate, tricarboxylic acid cycle, fatty acid oxidation, cellular movement, cellular proliferation and apoptosis. Furthermore, mitochondria are involved in altered metabolism in cancer cells. Several notable differences between normal cells and transformed cells have been discovered in their mitochondria (1).

Multidrug resistance (MDR) is a multi-factorial phenomenon and the major cause of chemotherapeutic failure in cancer therapy. MDR effectors include transporter glycoproteins such as P-glycoprotein/ABCB1, MRP1/ABCC1 and BCRP/ABCG2. It is known that the depletion of mitochondrial DNA (mtDNA) is relevant to tumorigenesis and multidrug resistance. However, whether and how mtDNA depletion affects the expression of molecules involved in drug resistance remains unclear.

It is implicated that mitochondria-mediated apoptosis is regulated by the B-cell lymphoma 2 (Bcl-2) family of apoptosis regulator proteins, including both anti-apoptotic and pro-apoptotic members. Two of the anti-apoptotic members, namely Bcl-2 and Bcl-xL, confer resistance to apoptosis induced by a number of stimuli, whereas pro-apoptotic proteins such as Bid, Bax, Bak and BH-3 domain-only proteins promote apoptosis (2,3). Therefore, the intracytosolic balance of members in the Bcl-2 family is critical for the maintenance of mitochondrial membrane integrity (4). Bcl-2 forms heterodimers with Bax *in vivo*, and prevents Bax from oligomerization and insertion into the mitochondrial membrane (5,6). Previous studies demonstrated that TNF-related apoptosis-inducing ligand (TRAIL) induced the translocation of Bax from cytosol to mitochondrial membrane in SK-Hep1 cells, and that the absence of this translocation was partly responsible for the resistance of the mitochondrial DNA-deficient cells (ϱ^0SK-Hep1) to TRAIL-induced apoptosis. However, SK-Hep1 and ϱ^0SK-Hep1 cells are both susceptible to antagonistic anti-Fas antibody (CH-11), TNFα or staurosporine (7,8).

MtDNA-depleted mammalian cell lines, defined as ϱ^0, can be induced by long-term culture in the presence of compounds such as ethidium bromide (EtBr) that damage mtDNA and inhibit mitochondrial replication (9). ϱ^0 cells and their cybrids are interesting models for investigating the influences of different mtDNA genomes (haplotypes) on a variety of cell functions. Because mitochondria are pivotal components of the apoptotic cell death machinery, ϱ^0 cells are also employed to study drug toxicity and cell death (10-13).

It has been shown that the overexpressions of P-glycoprotein (P-gp) and MDR-associated proteins (MRPs) such as MRP1 and MRP2 mediate pump-related multi-drug resistance in many different cancer cells (14,15). For examples, P-gp is expressed in the mitochondria of drug-resistant P1 (0.5) cells, but not in the mitochondria of drug-sensitive P5 cells (16). The release of cytochrome C from mitochondria to the cytosol is blocked in MDR cells, and this appears to be dependent on the overexpression of Bcl-xL (17). In this regard, mitochondrial expression of P-gp may protect the mitochondrial DNA from damage caused by anticancer drugs, and may be involved

Correspondence to: Dr Xianlong Ling, Department of Gastroenterology, Xinqiao Hospital, Third Military Medical University, Chongqing 400037, P.R. China
E-mail: docxianlong@yeah.net

*Contributed equally

Key words: mitochondrial DNA, tumor, multidrug resistance, P-glycoprotein

in the blockage of cytochrome C release into the cytosol in MDR cells. However, Munteanu *et al* (18) showed that in a human myeloid leukemia cell line (parental-sensitive cells and doxorubicin-resistant cells) K562, P-gp worked in the opposite direction by increasing the influx of anticancer drugs into the mitochondria.

We hypothesize that not only the expression of P-gp, but also those of Bcl-2 and Bax in the mitochondria interfere with apoptosis and multi-drug resistance. To elucidate the mechanism by which multi-drug resistance occurs, in this study, we investigate the role of mitochondria in doxorubicin-induced apoptosis, as well as mitochondrial expressions and localizations of Bcl-2, Bax and P-gp in whole cells and subcellular fractions using immunofluorescent confocal microscopy, flow cytometry and Western blot analyses.

Materials and methods

Reagents. Doxorubicin (DOX), cisplatin (DDP), vincristine (VCR), 5-fluorouridine (5-FU) and Rho123 were purchased from Sigma. MTT [3-(4,5-dimethylthiazol-2-yl)-2,5-diphenyl tetrazolium bromide] was obtained from Biomol. Anti-Bax, anti-Bcl-2, anti-P-gp, anti-MRP1 and anti-actin monoclonal antibodies were from Santa Cruz Biotechnology. MitoTracker Red CMXRos dye was purchased from Invitrogen. The Annexin V-FITC/PI apoptosis detection kit was from Nanjing KeyGen Biotech Co., Ltd. (Nanjing, China). Cell culture supplies were purchased from Corning Life Sciences (Lowell, MA, USA). Anti-tumor agents were prepared with complete culture medium immediately prior to use.

Cell lines and cultures. Human hepatoma cell line SK-Hep1 was obtained from the Institute of Biochemistry and Cell Biology, Chinese Academy of Life Sciences (Shanghai, China). The cells were grown in DMEM (Life Technologies) supplemented with 10% fetal bovine serum (FBS), 100 U/ml penicillin, and 100 μg/ml streptomycin in a humidified atmosphere of 5% CO_2 at 37˚C. Drug treatment was performed as described (19). Cell death was determined by trypan blue exclusion assay.

Derivation of ϱ^0 cells. SK-Hep1 cells were cultured in the presence of 100 ng/ml EtBr for >20 generations (ϱ^0 cells) (20). After 20 generations, mtDNA depletion was confirmed by PCR and Southern blot analysis (20,21). The ϱ^0SK-Hep1 cells were maintained in DMEM supplemented with 10% FBS, 50 μg/ml uridine and 100 μg/ml sodium pyruvate (ϱ^0 culture medium).

Fusion of ϱ^0SK-Hep1 cells with platelets. Human platelets were isolated according to a published procedure (22). Specifically, whole blood was heparinized at room temperature, mixed with 1/10 volume of 0.15 M NaCl and 0.1 M trisodium citrate (pH 7.0), and centrifuged at 150 x g for 14 min at 4˚C. The top 3/4 of platelet-rich plasma was removed and centrifuged at 2300 x g for 30 min at 4˚C. The pellet was re-suspended in 10 ml of physiological saline (0.15 M NaCl and 0.015 Tris-HCl buffer pH 7.4 at 25˚C). Platelets ($1x10^7$) and ϱ^0SK-Hep1 ($5x10^5$) cells were mixed in PBS and centrifuged at 160 x g for 5-10 min. The supernatant was aspirated and a polyethylene glycol solution [5 g PEG2000 (Amresco, USA), 1 ml 10% dimethylsulfoxide, and 4 ml DMEM] was added. After one minute, the suspension was diluted with 10 ml of DMEM supplemented with 10% FBS, 50 μg/ml uridine, and 100 μg/ml sodium pyruvate, and then distributed into five 25-ml culture flasks (Corning Costar, USA). Three days later, the uridine and pyruvate-containing medium was replaced with selective media (DMEM supplemented with 10% FBS, ϱ^0 test media). Individual clones were isolated three weeks after fusion (23).

Analysis of mitochondrial DNA

PCR. To compare the mtDNA content in parental, ϱ^0SK-Hep1 and SK-Hep1Cyb cells, total DNA was extracted using Omega E.Z.N.A. Tissue DNA Kit (Omega, USA) according to the manufacturer's instructions. PCR amplification of human mtDNA was performed in a 50-μl reaction mixture, which contained 0.25 units of Taq DNA polymerase (Takara, Japan), dNTP, template and 10 pmol each of the primers specific for human mtDNA (COX I and COX II) or human nuclear DNA (Table I). PCR was performed using a GeneAmp thermocycler (Perkin-Elmer) as follows: pre-denaturation for 5 min at 94˚C, and 30 cycles of denaturation for 30 sec at 94˚C, annealing for 30 sec at 55˚C, and extension for 60 sec at 72˚C, followed by a final extension of 10 min at 72˚C. PCR products were subjected to 1.1% agarose gel electrophoresis and stained with EtBr for examination.

Southern blot analysis. Total DNA (6 μg) was digested with *Eco*RI (New England BioLabs, Ipswich, MA) and fractionated by electrophoresis in a 0.8% agarose gel at 22 V for 18 h. DNA was transferred to nylon membranes (Ros). Biotin-labeled DNA probes were prepared using the North2South Biotin Random Prime Labeling Kit 17075 (Pierce, USA). Southern hybridization was performed according to the instructions of the North2 South Chemiluminescent Hybridization and Detection Kit 17097 (Pierce, USA).

Measurement of mitochondrial membrane potential ($\Delta\Psi_m$). Cells were grown on a slide at a density of $2x10^4$ cells/well in a six-well plate for 24 h, and incubated with corresponding culture media containing 200 nM MitoTracker Red for 30 min at 37˚C. After two washes in cold PBS, cells were fixed with 2% (w/v) paraformaldehyde in PBS at 4˚C for 20 min, and permeabilized with 0.5% (v/v) Triton X-100 in PBS for 15 min at room temperature. Slides were then washed twice with PBS, mounted and visualized under a Leica confocal laser scanning microscope (TCS SP2, Germany). For flow cytometry, cells ($5x10^5$/ml) were incubated with 200 nM MitoTracker Red for 30 min at 37˚C, harvested, and immediately analyzed with Coulter Epics XL flow cytometer (Beckman, USA).

MTT assay. The MTT viability assay was performed with slight modifications as previously described (24). The growth characteristics of SK-Hep1, ϱ^0SK-Hep1 and SK-Hep1Cyb cells were assessed in the same culture medium. Cells were seeded into 96-well plates at a density of $3x10^3$/well and cultured at 37˚C. After 24 h, cell number was calculated after trypan blue staining for five continuous days.

Cytotoxicity assay. Cytotoxic effects of doxorubicin were analyzed using MTT assay. Cells ($4x10^4$) were seeded in a 24-well plate and treated with various concentrations of doxorubicin (0, 0.01, 0.1, 1, 10 and 100 μg/ml) for 48 h. Cells were then trypsinized, harvested and enumerated after trypan blue

Table I. Primer sequences for COX I and COX II.

Primers		Sequences	Products (bp)
COX I	Upstream	5'-ACACGAGCATATTTCACCTCCG-3'	336
	Downstream	5'-GGATTTTGGCGTAGGTTTGGTC-3'	
COX II	Upstream	5'-ATCAAATCAATTGGCCACCAATGGTA-3'	297
	Downstream	5'-TTGACCGTAGTATACCCCCGGTC-3'	
β-actin	Upstream	5'-ACCACAGTCCATGCCATCAC-3'	500
	Downstream	5'-TCCACCACCCTGTTGCTGTA-3'	

β-actin was used as an internal control.

staining. Experiments were performed in triplicates, and the mean values, IC_{50} and RI were calculated (25). The cytotoxic effects of cisplatin, vincristine and 5-fluorouridine were evaluated using the same method.

Annexin V assay. Apoptosis was assayed with the Annexin V-FITC apoptosis detection kit according to the manufacturer's instructions. Briefly, $2x10^5$ cultured cells were collected, washed twice and re-suspended in 100 μl binding buffer, and then incubated with Annexin V-FITC at room temperature for 10 min followed by the addition of 6 μl propidium iodide (PI; 20 μg/ml) and incubation for 5 min. Fluorescent intensities were determined by flow cytometry.

Measurement of ROS production. To detect the production of ROS, cells were loaded with the membrane-permeable 2,7-dichlorofluorescein diacetate (DCFHDA), which was hydrolyzed to non-fluorescent DCFH that reacted with ROS to produce the highly fluorescent DCF. Cultured cells were incubated with or without 5.0 μg/ml doxorubicin for 8 h, followed by the addition of phenol red-free media containing 20 μM DCFHDA and incubation at 37˚C for 30 min. Cells were washed three times with PBS (pH 7.4) and analyzed using flow cytometry.

Preparation of mitochondrial fractions. Cells were washed twice with ice-cold PBS, and the pellet was suspended in 500 μl ice-cold buffer A (20 mM HEPES, pH 7.5, 1.5 mM $MgCl_2$, 10 mM KCl, 1 mM EDTA, 1 mM EGTA, 1 mM dithiothreitol, 0.1 mM phenylmethylsulfonyl fluoride, and 10 μg/ml each leupeptin, aprotinin and pepstatin A) containing 250 mM sucrose. To lyse the cells, the cell suspension was passed through a 26-gauge needle fitted to a syringe five times. The un-lysed cells, membrane debris and nuclei were removed by centrifuging the homogenates at 1000 x g for 10 min at 4˚C. The supernatant was subjected to 10,000 x g centrifugation for 20 min at 4˚C. The pellet fraction (i.e. mitochondria) was first washed with buffer A containing sucrose and then solubilized in 50 μl TNC buffer (10 mM Tris-acetate, pH 8.0, 0.5% Igepal CA-630, and 5 mM $CaCl_2$). The supernatant was re-centrifuged at 100,000 x g (4˚C, 1 h) to generate cytosol.

Immunofluorescence analysis. Cells were cultured on chamber slides, treated with doxorubicin for 8 h, washed with DMEM-10% FBS, and incubated in the corresponding media containing 100 nM MitoTracker Red for 30-45 min. Following incubation, cells were washed twice in PBS and fixed with 4% paraformaldehyde for 30 min at room temperature, and fixed in ice-cold 100% methanol for 10 min. Cells were washed three times with PBS, and non-specific binding was blocked with 2% horse serum-0.5% Triton X-100-0.02% NaN_3 in PBS for 20 min. Cells were then incubated with anti-Bax and anti-P-gp antibodies in PBS at room temperature for 90 min, and washed three times with PBS. Cells were then incubated with FITC and TRITC-conjugated secondary antibody for 40 min, washed three times with PBS and incubated with 4', 6-diamidino-2-phenylindole (DAPI) for 5 min. After three final washes with PBS, the slides were mounted for observation under a confocal laser scanning microscope and analyzed with the Leica TCS SP2 confocal laser imaging system (Leica Microsystems, Wetzlar, Germany).

SDS-PAGE and Western blot analysis. The cells were harvested, washed with PBS, re-suspended in 50 μl lysis buffer (20 mM HEPES, pH 7.4, 2 mM EGTA, 50 mM glycerophosphate, 1% Triton X-100, 10% glycerol, 1 mM PMSF, 10 μg/ml leupeptin, 10 μg/ml aprotinin and 10 μg/ml pepstatin), and incubated on ice for 30 min. After centrifugation at 20,000 rpm for 30 min at 4˚C, three volumes of Laemmli's sample buffer (0.625 M Tris-HCl pH 6.8, 10% β-mercaptoethanol, 20% SDS, 20% glycerol, and 0.004% bromophenol blue) was added to the supernatant and samples were boiled (100˚C) for 5 min. Proteins were separated by SDS-PAGE and transferred onto nitrocellulose membranes (Roche, USA). The membranes were probed with anti-Bcl-2, anti-Bax, anti-MRP1, anti-P-glycoprotein or anti-actin antibody in TBST buffer (10 mM Tris-HCl, 0.1 M NaCl, 0.1% Tween-20, pH 7.4) containing 5% skim milk overnight at 4˚C. Incubation with secondary antibodies conjugated with horseradish peroxidase was subsequently followed. The membranes were washed thrice with TBST. Immunoreactive bands were visualized by enhanced chemiluminescence (Cell Signal Biosciences), and the expression level of protein was determined using Image Quant TL software (Amersham Pharmacia Biotech).

Functional assay of mitochondrial P-gp. Mitochondrial fraction was prepared as described above. Mitochondria were suspended in buffer A and kept on ice until the experiment was performed (16). All imaging experiments were performed at room temperature in buffer A. Whole isolated mitochon-

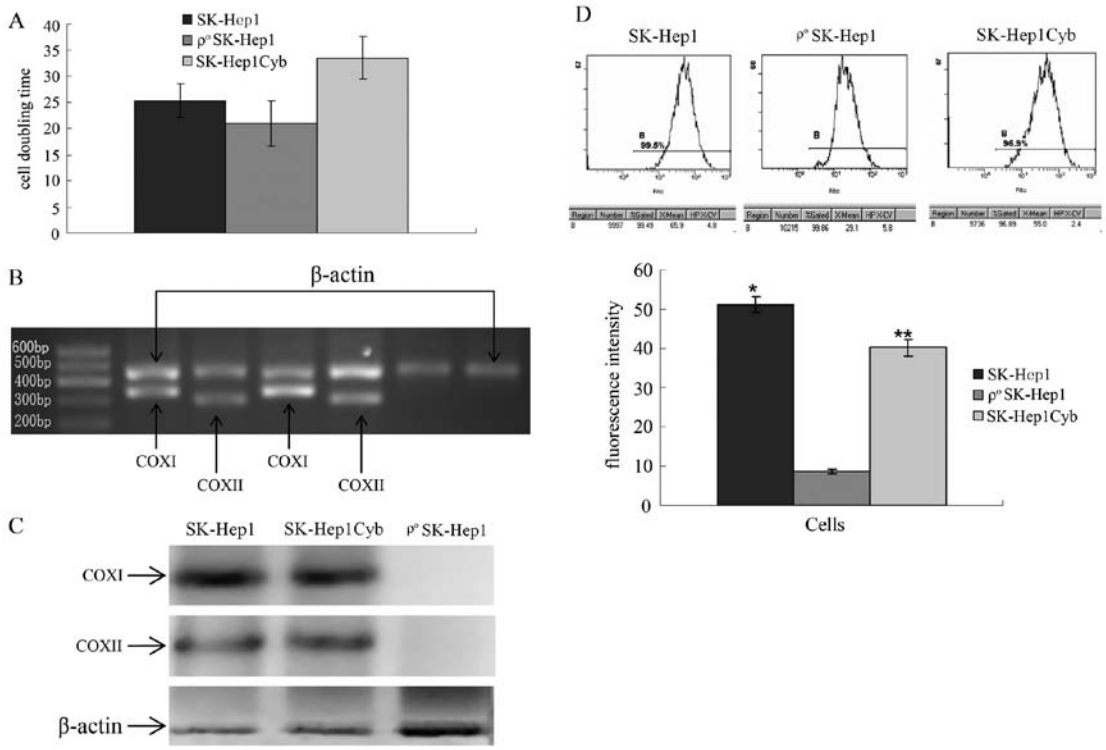

Figure 1. Establishment of ϱ^{0}SK-Hep1 and SK-Hep1Cyb cell lines and cell proliferation. (A) Compared with SK-Hep1 and SK-Hep1Cyb cells, ϱ^{0}SK-Hep1 cells had a reduced doubling time ($p<0.01$). SK-Hep1Cyb cells showed profoundly delayed growth kinetics compared to their parental cells ($p<0.01$). (B) PCR products of β-actin (500 bp) and mitochondrial COX I (336 bp) and COX II (297 bp) were visualized on agarose gel after EtBr staining. Marker (lane 1); SK-Hep1 cells (lanes 2 and 3); SK-Hep1Cyb cells (lanes 4 and 5); ϱ^{0}SK-Hep1 cells (lanes 6 and 7). (C) Southern blotting was performed with equal amounts of total DNA of SK-Hep1, ϱ^{0}SK-Hep1 and SK-Hep1Cyb cells. Using a probe for COX I/COX II, a 7.4-kb band was detected in the DNA from SK-Hep1 and SK-Hep1Cyb cells, but was absent in the DNA of ϱ^{0}SK-Hep1 cells. (D) Mitochondrial membrane potential of SK-Hep1, ϱ^{0}SK-Hep1 and SK-Hep1Cyb cells. The cells were stained with MitoTracker Red and fluorescent intensities of mitochondria were analyzed by flow cytometry. Data are expressed as the mean ± SEM of three independent experiments. $^*p=0.005<0.01$, vs. ϱ^{0}SK-Hep1. $^{**}p<0.01$, vs. SK-Hep1Cyb.

dria from cultured cells were divided in test tubes to evaluate mitochondrial autofluorescence as well as the uptake and the efflux of Rho123 into and out of organelles. Rho123 (5 μg/ml) was added to the samples and incubated for 4 min at room temperature in the dark. After incubation, fluorescence of Rho123 in mitochondria was measured by flow cytometry. To estimate Rho123 efflux, mitochondria exposed to Rho123 were re-suspended in 2 ml buffer A and centrifuged at 450 x g for 5 min at 4˚C. They were then washed once with 2 ml buffer A and diluted in 500 μl buffer A. Samples were incubated for an additional 6 min at room temperature to allow Rho123 efflux from the mitochondria. After incubation, the fluorescence of Rho123 in each sample was determined by flow cytometry and measured with a flow rate of 2,000 events/sec. At least three independent experiments were performed for each assay.

Statistical analysis. Data were expressed as mean ± SD (X ± S). Statistical analysis was performed with SPSS 13.0 software. Statistical significance between two groups was determined by paired or unpaired Student's t-test. Results for more than two experimental groups were evaluated by one-way ANOVA. A difference was considered statistically significant at $p<0.05$.

Results

Establishment of ϱ^{0}SK-Hep1 and SK-Hep1Cyb cell lines. To establish the mtDNA-depleted cell line, SK-Hep1 cells were treated with media containing 0.1 μg/ml EtBr, 100 μg/ml pyruvate and 50 μg/ml uridine for 10 weeks, and the cell doubling time decreased from 25 to 21 h (Fig. 1A). At that point, incubation in EtBr was discontinued. Viable cells were sub-cloned into EtBr-free (pyruvate/uridine supplemented) media. The clone, defined as ϱ^{0}SK-Hep1, was isolated and used in all the experiments described in this paper. This clone was then grown in ϱ^0 test media (Materials and methods) with a gradual decrease in number and viability after several doublings due to the loss of mtDNA (data not shown). The ϱ^{0}SK-Hep1 cells were auxotrophic for pyrimidines and pyruvate.

Total DNA was extracted from SK-Hep1 and ϱ^{0}SK-Hep1 cells. PCR demonstrated that mtDNA was amplified from total DNA of SK-Hep1 cells but not ϱ^{0}SK-Hep1 cells; while β-actin gene, a nuclear DNA control, was amplified from both SK-Hep1 and ϱ^{0}SK-Hep1 cells (Fig. 1B). For Southern hybridization, DNA was first digested with *Eco*RI, which was expected to cut mtDNA at three sites and produce three mtDNA fragments including the 7366-bp cytochrome C oxidase subunit gene. A probe for COX I and COX II detected a 7.4-kb band in DNA from SK-Hep1 cells but not in DNA from ϱ^{0}SK-Hep1 cells (Fig. 1C). These observations demonstrated that the ϱ0SK-Hep1 cells were entirely devoid of mtDNA (ϱ^0 cells). ϱ0SK-Hep1 cells were fused with platelets to obtain cybrids (SK-Hep1Cyb) and the mtDNA was detected both by PCR and Southern blot analysis in these cells (Fig. 1B and C)

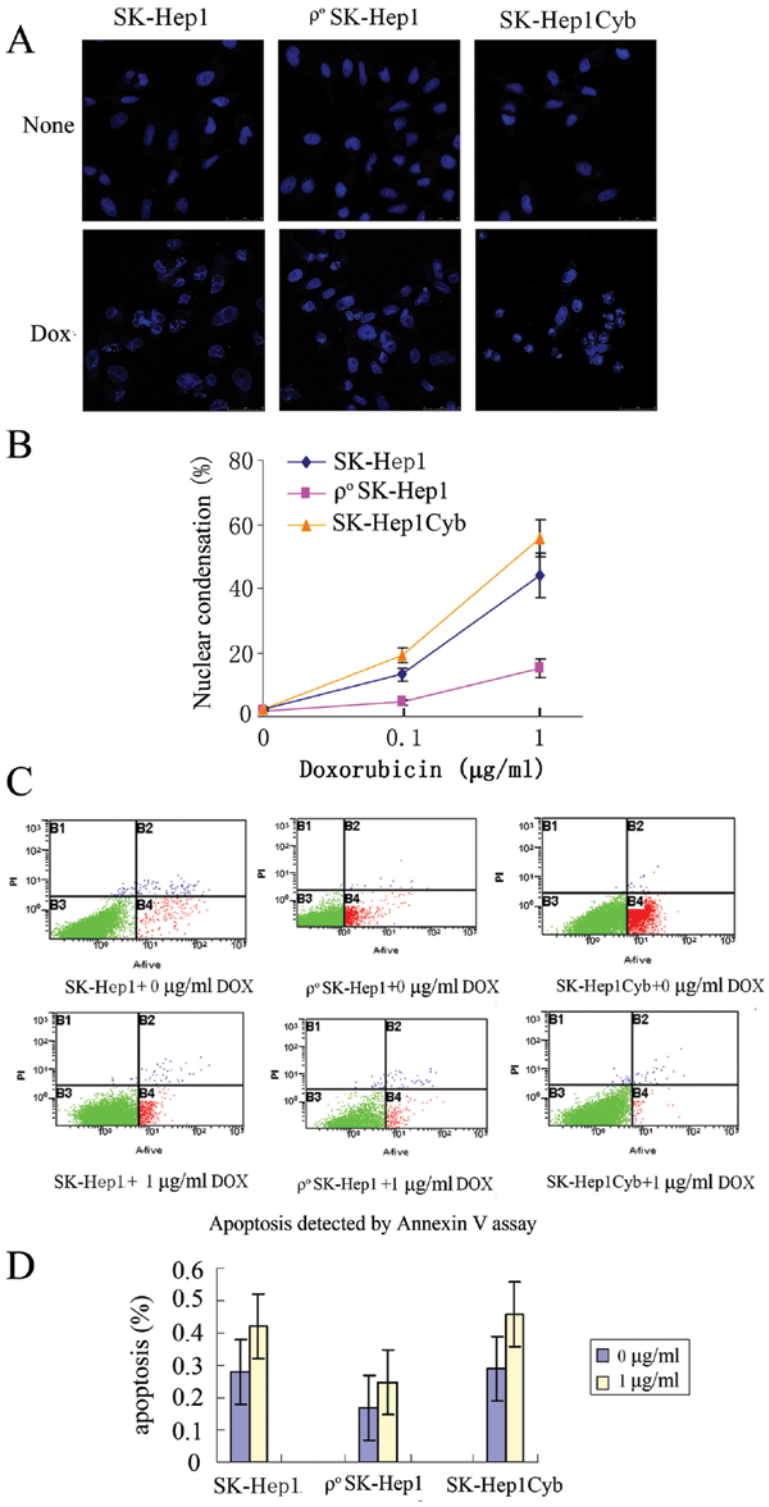

Figure 2. Cytotoxicity of doxorubicin on cultured cells. (A) SK-Hep1, ϱ0SK-Hep1 and SK-Hep1Cyb cells were incubated in the media containing different concentrations of doxorubicin for 48 h. Then cells were stained with DAPI (blue) for 5 min, fixed and detected using fluorescent microscopy. Cells with condensed or fragmented nuclei were considered as apoptotic cells. (B) Percentage of cells with increased nucleus condensation or fragmentation was calculated by counting at least 300 cells in 40-50 fields. Doxorubincin treatment led to typical signs of apoptosis in SK-Hep1 and SK-Hep1Cyb cells in a dose-dependent manner. However, ϱ^{0}SK-Hep1 cells were more resistant to doxorubincin-induced apoptosis. Annexin V assay showed similar results to DAPI staining.

Loss of $\Delta\Psi_m$ in ϱ^0 cells. Mitochondrial membrane potential was measured by flow cytometry using a MitoTracker Red flourescent probe. MitoTracker Red specifically detected mitochondrial inner membrane, and the intensity was greater with the increase of mitochondria membrane potential. ϱ^{0}SK-Hep1 cells lost mitochondrial membrane potential due to mtDNA depletion (P<0.01) (Fig. 1D).

Cytotoxicity of drugs in human hepatoma cells. As shown in Table II, when doxorubicin was used to treat SK-Hep1,

Table II. Multi-drug resistance index and IC_{50}.

Drugs	IC_{50} (μg/ml)			Resistance index	
	SK-Hep1	ϱ^{0}SK-Hep1	SK-Hep1Cyb	$RI^a_{ϱ°SK-Hep1}$	$1/RI^b_{SK-Hep1Cyb}$
DOX	0.62±0.02	4.93±0.17	0.57±0.02	7.95	1.05
DDP	5.04±0.06	16.34±0.29	2.02±0.12	3.24	2.49
VCR	0.77±0.03	0.87±0.03	0.63±0.02	1.13	1.22
5-FU	12.49±0.27	19.33±0.21	10.27±0.34	1.55	1.22

[a]p<0.01, ϱ^{0}SK-Hep1 vs. SK-Hep1; [b]p>0.05, SK-Hep1Cyb vs. SK-Hep1.

ϱ^{0}SK-Hep1 and SK-Hep1Cyb cells, the IC_{50} values were 0.62, 4.93 and 0.57 μg/ml, respectively. The RI of ϱ^{0}SK-Hep1 cells was 7.95 times greater than that of SK-Hep1 cells. SK-Hep1Cyb cells had no detectable resistance, and the 1/RI of SK-Hep1Cyb cells was 1.05 times greater than that of SK-Hep1 cells. The ϱ^{0}SK-Hep1 cells had the highest drug resistance to DDP, followed by SK-Hep1Cyb and SK-Hep1 cells. Repletion of mtDNA into ϱ^{0}SK-Hep1 cells restored the susceptibility to doxorubicin and DDP, but not to other agents. None of the cells had detectable resistance to VCR and 5-FU (Table II). Doxorubicin treatment led to typical signs of apoptosis in SK-Hep1 and SK-Hep1Cyb cells (Fig. 2A). After 48 h of incubation with increasing concentrations of doxorubicin (0, 0.1 and 1 μg/ml), the viabilities of SK-Hep1 and SK-Hep1Cyb cells decreased in a dose-dependent manner (Fig. 2B). DAPI staining showed nuclear chromatin condensation and fragmentation into apoptotic bodies. ϱ^{0}SK-Hep1 cells were more resistant to doxorubicin-induced apoptosis (Fig. 2A). The results suggested that the percentage of apoptotic cells in ϱ^{0}SK-Hep1 was significantly higher than those in SK-Hep1 and SK-Hep1Cyb (P<0.01). Similar results were obtained using the Annexin V assay (Fig. 2C and D). In addition, SK-Hep1Cyb cells showed reverse resistance to doxorubicin when compared with SK-Hep1 (P<0.05) (Fig. 2C).

Bax translocation and ROS generation were inhibited in ϱ^{0}SK-Hep1 cells. Western blot analyses showed that Bcl-2 and Bax were both overexpressed in mtDNA-depleted cells (ϱ^{0}SK-Hep1 cells) (Fig. 3A), which was in agreement with the results of previous reports (6,7). However, the expression level of anti-apoptotic Bcl-2 was lower, and the expression level of pro-apoptotic Bax was higher in the cybrids SK-Hep1Cyb cells when compared with those in SK-Hep1 and ϱ^{0}SK-Hep1 cells. Korsmeyer *et al* (26) demonstrated that a pre-set ratio of Bcl-2/Bax determined the survival or death of cells following an apoptotic stimulus. We found that the Bcl-2/Bax ratio was the highest in ϱ^{0}SK-Hep1 cells, but was the lowest in SK-Hep1Cyb cells (Fig. 3B), which might partly contribute to the multi-drug resistance of ϱ^{0}SK-Hep1 cells.

Immunofluorescent analyses were performed to investigate the localization of Bax in untreated and doxorubicin-treated cells. In SK-Hep1 and SK-Hep1Cyb cells, Bax was diffusely distributed before doxorubicin treatment (Fig. 4A). However, after 6 h of doxorubicin treatment, Bax redistributed from cytosol to the mitochondria (27) (Fig. 4A). A large proportion of the SK-Hep1 and SK-Hep1Cyb cells displayed a punctuated

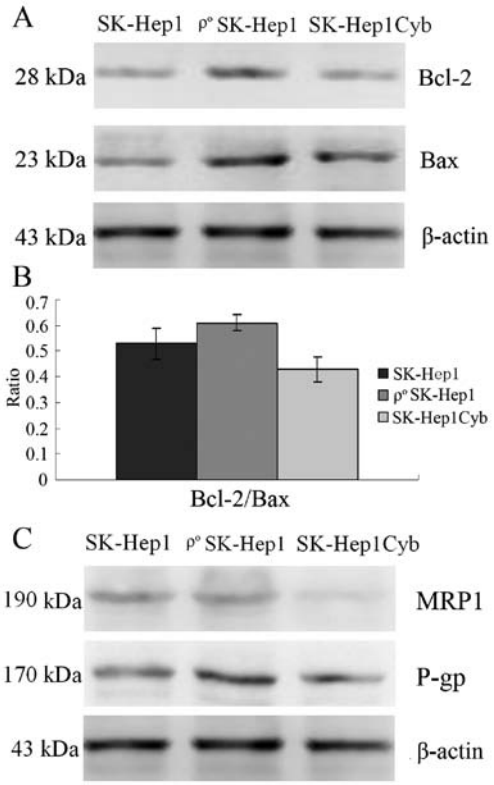

Figure 3. Western blot analyses of P-gp, MRP1, Bcl-2 and Bax in different cell lines. (A) SK-Hep1, ϱ^{0}SK-Hep1 and SK-Hep1Cyb cells were harvested for the detection of P-gp, MRP1, Bcl-2 and Bax by immunoblot using anti-P-gp, anti-MRP1, anti-Bcl-2 and anti-Bax antibody, respectively. β-actin served as a loading control. (B) Bcl-2 and Bax expressions were up-regulated in ϱ^{0}SK-Hep1 cells with significantly increased Bcl-2/Bax ratio. (C) P-gp and MRP1 expressions were up-regulated in ϱ^{0}SK-Hep1 cells, but down-regulated in SK-Hep1Cyb cells.

mitochondrial pattern of Bax immunostaining, suggesting that the translocation of Bax might facilitate its recognition by the anti-Bax antibody. In ϱ^{0}SK-Hep1 cells, Bax translocation was not detected as in SK-Hep1 and SK-Hep1Cyb cells. Triple-colored staining with a mitochondria-selective dye MitoTracker Red, DAPI (data not shown) and anti-Bax antibody confirmed that Bax was indeed localized to the mitochondria in SK-Hep1, ϱ^{0}SK-Hep1 and SK-Hep1Cyb cells. These results suggested that the low amount of Bax translocation was responsible for the lack of doxorubicin sensitivity in ϱ^{0}SK-Hep1 cells.

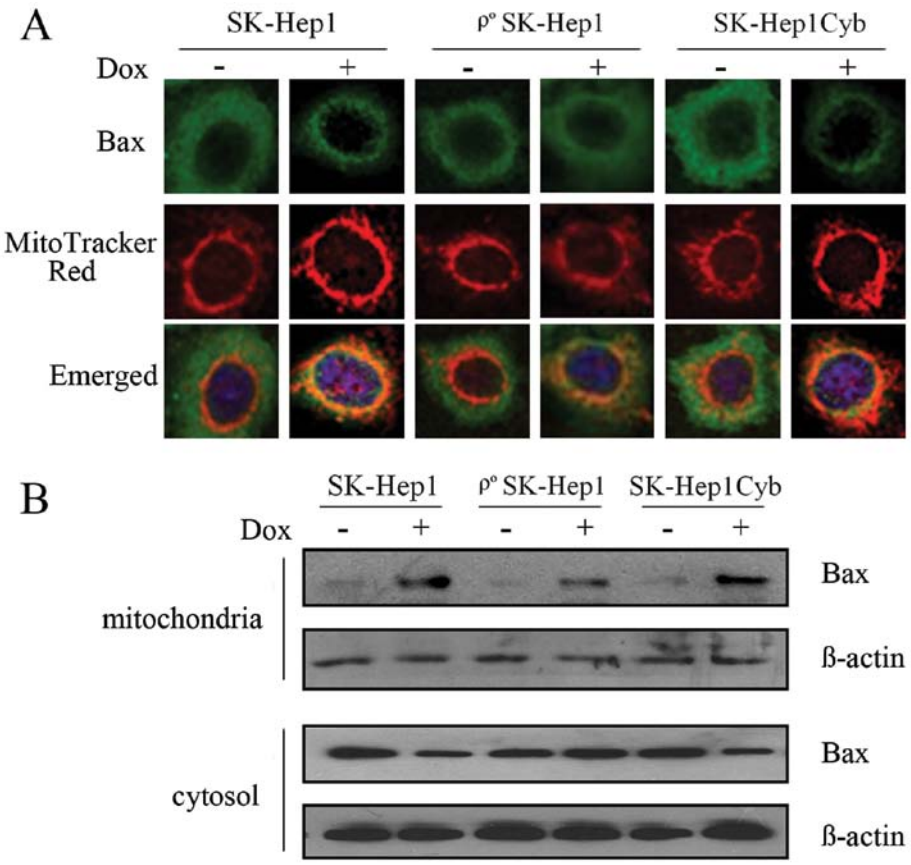

Figure 4. Bax translocation were inhibited in ϱ^{0}SK-Hep1 cells. (A) SK-Hep1, ϱ^{0}SK-Hep1 and SK-Hep1Cyb cells were incubated with 200 nm MitoTracker Red for 15 min, fixed and immunostained with anti-Bax antibody. Next, samples were stained with FITC-labeled secondary antibody (green) and DAPI (blue) and subjected to confocal microscopy. Representative images are shown. Scale bars are 10 μm. (B) Protein extracts (50 μg) were separated on a 12% SDS-PAGE gel and immunoblotted as described in Materials and methods. Bax expression was decreased in the cytosolic fraction but increased in the heavy membrane fraction of the parental and SK-Hep1Cyb cells after 6 h of 5.0 μg/ml doxorubicin treatment. Only small quantities of Bax translocation were detected in ϱ^{0}SK-Hep1 cells after doxorubicin treatment.

Table III. Accumulation and efflux of Rho123 in SK-Hep1, ϱ^{0}SK-Hep1 and SK-Hep1Cyb cells detected by flow cytometry.

Cells	Rho123 accumulation	Rho123 efflux
SK-Hep1	41.5±1.2	27.4±2.4
ϱ^{0}SK-Hep1	28.2±2.1[a]	16.5±1.2[a]
SK-Hep1Cyb	42.9±2.3	29.5±3.1

[a]p<0.05, vs. SK-Hep1 and SK-Hep1Cyb cells.

The expression of Bax was decreased in the cytosolic fraction, but increased in the heavy membrane fraction when SK-Hep1 and SK-Hep1Cyb cells were treated with 5.0 μg/ ml doxorubicin for 6 h (Fig. 4B), indicating that doxorubicin induced the translocation of Bax from cytosolic fraction to heavy membrane fraction. However, the expression of Bax remained stationary in cytosolic fraction of ϱ^{0}SK-Hep1 cells before and after doxorubicin treatment, and only a small amount of Bax translocation to heavy membrane fraction was observed after doxorubicin treatment (Fig. 4B). After 6 h of doxorubicin treatment, the fluorescent intensity of DCF increased significantly in parental and cybrid cells but not in ϱ^0 cells, suggesting that doxorubicin enhanced the production of radical oxygen species (ROS) in cells with intact mitochondrial function but not in mitochondrial DNA-depleted cells (Fig. 5).

Expression levels of P-gp and MRP1 were increased in ϱ^{0}SK-Hep1 cells and P-gp was localized in the mitochondria. Western blot analysis showed that the expressions of P-gp and MRP1 were higher in ϱ^{0}SK-Hep1 cells than those in SK-Hep1 and SK-Hep1Cyb cells, and that MRP1 expression was lower in SK-Hep1Cyb cells than those in ϱ^{0}SK-Hep1 and SK-Hep1 cells (Figs. 3C and 6). Immunofluorescent analysis showed that P-gp was localized in the mitochondria of all three cell lines (Fig. 6).

P-gp-mediated accumulation and efflux of Rho123. To demonstrate whether P-gp in the mitochondria was functionally active or not, we measured the accumulation and efflux of the fluorescent dye Rho123. Compared with SK-Hep1 cells, Rho123 accumulation in the mitochondria was reduced in ϱ^{0}SK-Hep1 cells, but restored to a similar level in the cybrids cells (Table III). Once Rho123 was removed from the incubation mixture, fluorescent intensity decreased faster in the mitochondria of ϱ^{0}SK-Hep1 cells than in those of SK-Hep1 cells.

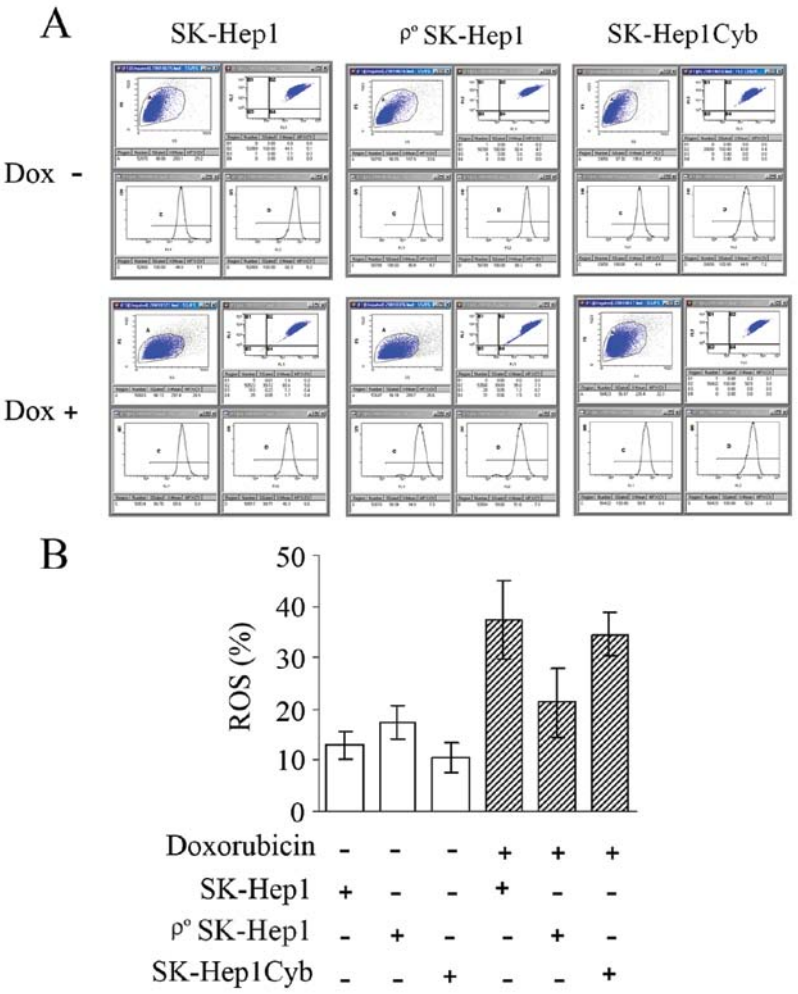

Figure 5. ROS is inhibited in ρ^0SK-Hep1 cells. Cells were treated with 5.0 μg/ml DOX for 0 (top) and 8 h (bottom). ROS production was detected with 2,7-dichlorofluorescein diacetate (DCFHDA). ROS production in parental and cybrid cells were about two times more than that of ρ^0 cells ($p<0.01$), but the difference between parental and cybrid cells was not significant ($p>0.05$).

Discussion

Although Bax translocation was observed in ρ^0SK-Hep1 cells after doxorubicin treatment in our study, it was not adequate for apoptosis to occur. The translocation of Bax to mitochondria has been reported in several apoptosis models including those induced by TNF, staurosporine and cisplatin (27-30). The mechanism of the decreased Bax translocation in doxorubicin-treated ρ^0 cells remains unclear. Uncontrollable production of ROS triggers the opening of the mitochondrial permeability transition pore and induces apoptosis and/or necrosis (31-33). Our experiments suggest that decreased ROS generation following doxorubicin treatment in ρ^0 cells is likely responsible for the Bax translocation insufficiency and resistance to doxorubicin.

Activations of Bax and Bak are critical to the permeabilization of the outer mitochondrial membrane. Cytochrome C is released from mitochondria into the cytosol (12,34,35). This release is suppressed by Bcl-2 in the mitochondrial. Mitochondrial Bcl-2 blocks the activation of Bax during ATP depletion, which is a critical event for mitochondrial outer membrane permeabilization and cytochrome C release. Bcl-2 heterodimerizes with Bax *in vivo*, and prevents Bax oligomerization and its insertion into the mitochondrial membrane (5,6). Characterized by the presence of Bcl-2 homology (BH) domains, these proteins can be pro-apoptotic or anti-apoptotic. In our study, ρ^0SK-Hep1 cells had a loss of $\Delta\Psi_m$, and were more resistant to doxorubicin than SK-Hep1 cells. But after repletion of mtDNA, the sensitivity of the ρ^0SK-Hep1 cells to doxorubicin was restored. After SK-Hep1, ρ^0SK-Hep1 and SK-Hep1Cyb cells were treated with 5.0 μg/ml doxorubicin for 4 and 8 h, typical signs of apoptosis were induced in SK-Hep1 and SK-Hep1Cyb cells, and ROS generation was also increased.

P-gp functions as a pump and extrudes anticancer drugs and other compounds from the cells (14,36,37). MDR can be intrinsic or acquired during chemotherapy, and is characterized by the fact that cells show cross-resistance to a variety of structurally and functionally unrelated drugs (38). The overexpression of P-gp and MRPs, such as MRP1 and MRP2, are the main causes of pump-related multidrug resistance in different cancer cells (14,15). Mitochondrial expression of P-gp protects the mitochondrial DNA from damage caused by anticancer drugs, and might be involved in the mechanism by which MDR cells block the release of cytochrome C into cytosol, which appears to be dependent on the overexpression of Bcl-xL. Because the overexpression of P-gp blocks

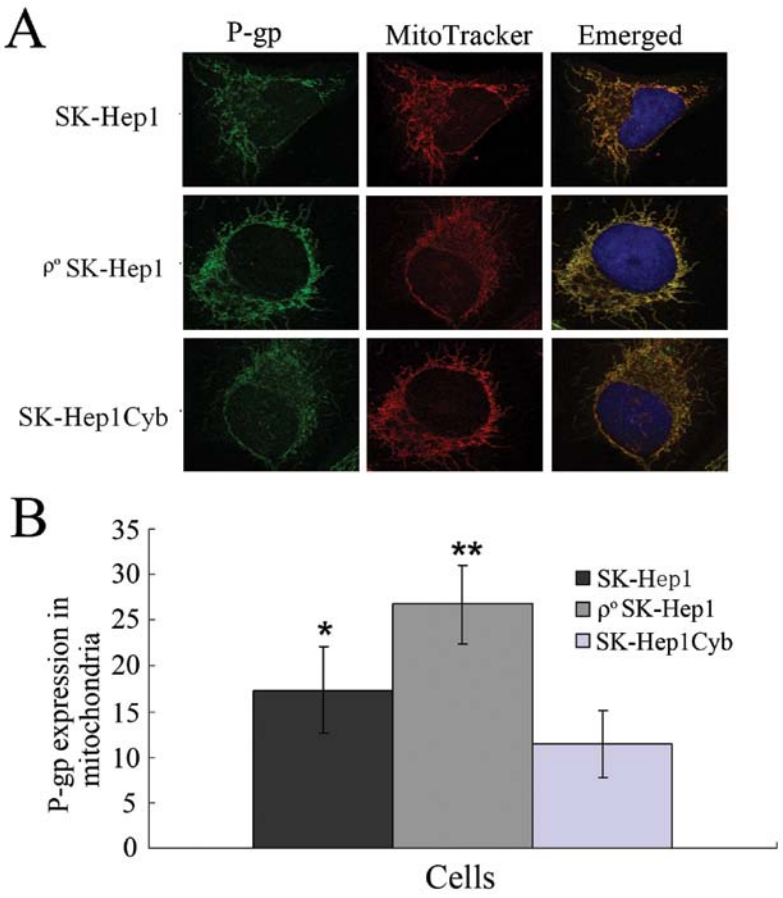

Figure 6. P-gp localization in mitochondria. SK-Hep1, ϱ^0SK-Hep1 and SK-Hep1Cyb cells were incubated with 200 nm MitoTracker Red for 15 min, fixed and immunostained with anti-P-gp antibody. Next, samples were stained with FITC-labeled secondary antibody (green) and DAPI (blue) and subjected to confocal microscopy. Representative images are shown. Scale bars are 10 μm. $^{*}p<0.05$, vs. SK-Hep1Cyb. $^{**}p<0.01$, vs. SK-Hep1.

the release of cytochrome C into the cytosol after apoptotic stimuli, it is tempting to hypothesize that drugs inhibiting the MDR phenotype may also reverse the release of cytochrome C and thus revert the drug-resistance. Minko *et al* (39) demonstrate that resistant MCF-7 cells treated with doxorubicin alone have increased levels of Bcl-2. A related study shows that verapamil treatment preferentially induces apoptosis in MDR cells and the overexpression of Bcl-2 inhibits this apoptosis (40). The overexpression of Bax proteins sensitizes cancer cells to several chemotherapeutic agents (41). Bcl-2 overexpression in tumor cells results in MDR to a broad spectrum of anticancer drugs and is correlated with a poor response to chemotherapy in many human cancers (42). We show here an increased expression of anti-apoptotic activity (Bcl-2 overexpression) and a significant overexpression of pro-apoptotic signal (Bax expression) in ϱ^0 cells. However, in SK-Hep1Cyb cells, the expression of Bcl-2 is decreased, and the expression of Bax is higher than that in parental cells. An increase in Bcl-2/Bax ratio may represent the inactivation of a pro-apoptotic mitochondria-derived signal. There might be functional P-gp localization to the mitochondria, which is responsible for the changes in the expressions of Bcl-2 and Bax and the resistance to doxorubicin-induced apoptosis in ϱ^0SK-Hep1 cells. We have observed insufficient Bax translocation in ϱ^0 cells. The above partly explain the resistance to doxorubicin-induced apoptosis of ϱ^0SK-Hep1 cells.

In addition to efflux pump activity, P-gp and MRPs are also involved in augmenting tumor cell survival by protecting drug-resistant cells from anticancer drug, Fas ligand, TNF-α, and UV irradiation-mediated activation of caspase-dependent apoptosis. Accordingly, the up-regulation of P-gp is associated with the overexpression of the anti-apoptotic Bcl family proteins (43) and the inhibitions of caspase-8 and caspase-3 (39).

To investigate the mitochondrial P-gp function, accumulation and efflux of Rho123, a mitochondrion fluorescent probe with strong analogy with anticancer drugs were evaluated in isolated mitochondria from parental cells, ϱ^0 cells and the cybrids cells. Results of these experiments completely agree with those obtained in whole cells. Rho123 accumulation is significantly reduced in isolated mitochondria of ϱ^0 cells compared to their parental cells. The reduced mitochondrial fluorescence of ϱ^0 cells is probably due to the P-gp-mediated Rho123 efflux.

In conclusion, our study reveals that ϱ^0SK-Hep1 cells are resistant to both doxorubicin and cisplatin, while cybrids (SK-Hep1Cyb) exhibit restored susceptibility to both drugs. Bax translocation to mitochondrial membrane is partly inhibited in ϱ^0 cells with an increased Bcl-2/Bax, suggesting that a depletion of mitochondrial DNA may contribute to MDR by developing apoptotic resistance in hepatoma cells. In addition, the overexpressions of P-gp and MRP1 are found in ϱ^0 cells, and P-gp has mitochondria localization in all three of these

cell lines. However, the function of P-gp localization to the mitochondria requires further investigation.

Acknowledgements

This work was supported by grants from National Natural Science Foundation of China (no. 30470865) and Xinqiao Hospital Foundation (no. 1520).

Reference

1. Modica-Napolitano JS, Kulawiec M and Singh KK: Mitochondria and human cancer. Curr Mol Med 7: 121-131, 2007.
2. Borner C: The Bcl-2 protein family: sensors and checkpoints for life-or-death decisions. Mol Immunol 39: 615-647, 2003.
3. Danial NN and Korsmeyer SJ: Cell death: critical control points. Cell 116: 205-219, 2004.
4. Shrivastava A, Tiwari M, Sinha RA, *et al*: Molecular iodine induces caspase-independent apoptosis in human breast carcinoma cells involving the mitochondria-mediated pathway. J Biol Chem 281: 19762-19771, 2006.
5. Oltvai ZN, Milliman CL and Korsmeyer SJ: Bcl-2 heterodimerizes in vivo with a conserved homolog, Bax, that accelerates programmed cell death. Cell 74: 609-619, 1993.
6. Antonsson B, Montessuit S, Sanchez B and Martinou JC: Bax is present as a high molecular weight oligomer/complex in the mitochondrial membrane of apoptotic cells. J Biol Chem 276: 11615-11623, 2001.
7. Kim JY, Kim YH, Chang I, *et al*: Resistance of mitochondrial DNA-deficient cells to TRAIL: role of Bax in TRAIL-induced apoptosis. Oncogene 21: 3139-3148, 2002.
8. Lee MS, Kim JY and Park SY: Resistance of rho(0) cells against apoptosis. Ann NY Acad Sci 1011: 146-153, 2004.
9. King MP and Attardi G: Human cells lacking mtDNA: repopulation with exogenous mitochondria by complementation. Science 246: 500-503, 1989.
10. Jacobson MD, Burne JF, King MP, Miyashita T, Reed JC and Raff MC: Bcl-2 blocks apoptosis in cells lacking mitochondrial DNA. Nature 361: 365-369, 1993.
11. Jiang S, Cai J, Wallace DC and Jones DP: Cytochrome c-mediated apoptosis in cells lacking mitochondrial DNA. Signaling pathway involving release and caspase 3 activation is conserved. J Biol Chem 274: 29905-29911, 1999.
12. Wang J, Silva JP, Gustafsson CM, Rustin P and Larsson NG: Increased in vivo apoptosis in cells lacking mitochondrial DNA gene expression. Proc Natl Acad Sci USA 98: 4038-4043, 2001.
13. Liu CY, Lee CF, Hong CH and Wei YH: Mitochondrial DNA mutation and depletion increase the susceptibility of human cells to apoptosis. Ann NY Acad Sci 1011: 133-145, 2004.
14. Gottesman MM and Pastan I: Biochemistry of multidrug resistance mediated by the multidrug transporter. Annu Rev Biochem 62: 385-427, 1993.
15. Lo YL: Relationships between the hydrophilic-lipophilic balance values of pharmaceutical excipients and their multidrug resistance modulating effect in Caco-2 cells and rat intestines. J Control Release 90: 37-48, 2003.
16. Solazzo M, Fantappie O, Lasagna N, Sassoli C, Nosi D and Mazzanti R: P-gp localization in mitochondria and its functional characterization in multiple drug-resistant cell lines. Exp Cell Res 312: 4070-4078, 2006.
17. Kojima H, Endo K, Moriyama H, *et al*: Abrogation of mitochondrial cytochrome c release and caspase-3 activation in acquired multidrug resistance. J Biol Chem 273: 16647-16650, 1998.
18. Munteanu E, Verdier M, Grandjean-Forestier F, *et al*: Mitochondrial localization and activity of P-glycoprotein in doxorubicin-resistant K562 cells. Biochem Pharmacol 71: 1162-1174, 2006.
19. Li YZ, Lu DY, Tan WQ, Wang JX and Li PF: p53 initiates apoptosis by transcriptionally targeting the antiapoptotic protein ARC. Mol Cell Biol 28: 564-574, 2008.
20. Park KS, Nam KJ, Kim JW, *et al*: Depletion of mitochondrial DNA alters glucose metabolism in SK-Hep1 cells. Am J Physiol Endocrinol Metab 280: E1007-E1014, 2001.
21. Armand R, Channon JY, Kintner J, *et al*: The effects of ethidium bromide induced loss of mitochondrial DNA on mitochondrial phenotype and ultrastructure in a human leukemia T-cell line (MOLT-4 cells). Toxicol Appl Pharmacol 196: 68-79, 2004.
22. Mann VM, Cooper JM, Krige D, Daniel SE, Schapira AH and Marsden CD: Brain, skeletal muscle and platelet homogenate mitochondrial function in Parkinson's disease. Brain 115: 333-342, 1992.
23. Chomyn A, Lai ST, Shakeley R, Bresolin N, Scarlato G and Attardi G: Platelet-mediated transformation of mtDNA-less human cells: analysis of phenotypic variability among clones from normal individuals-and complementation behavior of the tRNALys mutation causing myoclonic epilepsy and ragged red fibers. Am J Hum Genet 54: 966-974, 1994.
24. Mosmann T: Rapid colorimetric assay for cellular growth and survival: application to proliferation and cytotoxicity assays. J Immunol Methods 65: 55-63, 1983.
25. Snow K and Judd W: Characterisation of adriamycin- and amsacrine-resistant human leukaemic T cell lines. Br J Cancer 63: 17-28, 1991.
26. Korsmeyer SJ, Shutter JR, Veis DJ, Merry DE and Oltvai ZN: Bcl-2/Bax: a rheostat that regulates an anti-oxidant pathway and cell death. Semin Cancer Biol 4: 327-332, 1993.
27. Wolter KG, Hsu YT, Smith CL, Nechushtan A, Xi XG and Youle RJ: Movement of Bax from the cytosol to mitochondria during apoptosis. J Cell Biol 139: 1281-1292, 1997.
28. Qian W, Nishikawa M, Haque AM, *et al*: Mitochondrial density determines the cellular sensitivity to cisplatin-induced cell death. Am J Physiol Cell Physiol 289: C1466-C1475, 2005.
29. Hsu YT, Wolter KG and Youle RJ: Cytosol-to-membrane redistribution of Bax and Bcl-X(L) during apoptosis. Proc Natl Acad Sci USA 94: 3668-3672, 1997.
30. Perez D and White E: TNF-alpha signals apoptosis through a bid-dependent conformational change in Bax that is inhibited by E1B 19K. Mol Cell 6: 53-63, 2000.
31. Green DR and Reed JC: Mitochondria and apoptosis. Science 281: 1309-1312, 1998.
32. Kroemer G and Reed JC: Mitochondrial control of cell death. Nat Med 6: 513-519, 2000.
33. Kallio A, Zheng A, Dahllund J, Heiskanen KM and Harkonen P: Role of mitochondria in tamoxifen-induced rapid death of MCF-7 breast cancer cells. Apoptosis 10: 1395-1410, 2005.
34. Dong Z and Wang J: Hypoxia selection of death-resistant cells. A role for Bcl-X(L). J Biol Chem 279: 9215-9221, 2004.
35. Mikhailov V, Mikhailova M, Pulkrabek DJ, Dong Z, Venkatachalam MA and Saikumar P: Bcl-2 prevents Bax oligomerization in the mitochondrial outer membrane. J Biol Chem 276: 18361-18374, 2001.
36. Germann UA: P-glycoprotein-a mediator of multidrug resistance in tumour cells. Eur J Cancer 32: 927-944, 1996.
37. Mazzanti R, Croop JM, Gatmaitan Z, *et al*: Benzquinamide inhibits P-glycoprotein mediated drug efflux and potentiates anticancer agent cytotoxicity in multidrug resistant cells. Oncol Res 4: 359-365, 1992.
38. Breier A, Barancik M, Sulova Z and Uhrik B: P-glycoprotein-implications of metabolism of neoplastic cells and cancer therapy. Curr Cancer Drug Targets 5: 457-468, 2005.
39. Minko T, Batrakova EV, Li S, *et al*: Pluronic block copolymers alter apoptotic signal transduction of doxorubicin in drug-resistant cancer cells. J Control Release 105: 269-278, 2005.
40. Karwatsky J, Lincoln MC and Georges E: A mechanism for P-glycoprotein-mediated apoptosis as revealed by verapamil hypersensitivity. Biochemistry 42: 12163-12173, 2003.
41. Miao ZH, Tang T, Zhang YX, Zhang JS and Ding J: Cytotoxicity, apoptosis induction and downregulation of MDR-1 expression by the anti-topoisomerase II agent, salvicine, in multidrug-resistant tumor cells. Int J Cancer 106: 108-115, 2003.
42. Buchholz TA, Davis DW, McConkey DJ, *et al*: Chemotherapy-induced apoptosis and Bcl-2 levels correlate with breast cancer response to chemotherapy. Cancer J 9: 33-41, 2003.
43. Campone M, Vavasseur F, Le Cabellec MT, Meflah K, Vallette FM and Oliver L: Induction of chemoresistance in HL-60 cells concomitantly causes a resistance to apoptosis and the synthesis of P-glycoprotein. Leukemia 15: 1377-1387, 2001.